Published in final edited form as:
Arch Biochem Biophys. 2013 December ; 540(0): 94–100. doi:10.1016/j.abb.2013.10.012.

14-3-3ε and NAV2 interact to regulate neurite outgrowth and axon elongation

Mark A. Marzinke[†], **Terri Mavencamp**[†], **Joseph Duratinsky**[†], and **Margaret Clagett-Dame**[†,‡]

[†]Department of Biochemistry, College of Agricultural and Life Sciences, University of Wisconsin-Madison, Madison, WI

[‡]Pharmaceutical Sciences Division, School of Pharmacy, University of Wisconsin-Madison, Madison, WI

Abstract

Neuron navigator 2 (NAV2) is required for all-*trans* retinoic acid (atRA) to induce neurite outgrowth in human neuroblastoma cells. Further, ectopic overexpression of full-length human *NAV2* rescues an axonal elongation defect in the *C. elegans unc-53* (NAV2 ortholog) mutant. Using a region of NAV2 that independently associates with the cytoskeleton as bait in a yeast-two-hybrid screen, 14-3-3ε was identified as a novel NAV2 interacting partner. Amino acids 761–936 of NAV2 are sufficient to confer a positive interaction with 14-3-3ε as evidenced by a two-hybrid screen and co-immunoprecipitation assay. Knockdown of 14-3-3ε leads to a decrease in atRA-mediated neurite outgrowth, similar to the elongation defects observed when NAV2 is depleted or mutated. Likewise, posterior lateral microtubule (PLM) defects in *C. elegans* fed *unc-53* RNAi are similar to those fed *ftt-2* (14-3-3 homolog) RNAi. The discovery of an interaction between NAV2 and 14-3-3ε could provide insight into the mechanism by which NAV2 participates in promoting cell migration and neuronal elongation.

Introduction

Neuron navigator 2 (*NAV2*, also known as retinoic-acid induced in neuroblastoma-1; *RAINB1*, *POMFIL1*, *HELAD1*, *unc53H2*) functions in neurite outgrowth and axonal elongation in organisms ranging from *Caenorhabditis elegans* (*C. elegans*) to humans [1–4]. *NAV2* was initially discovered as a gene induced by all-*trans* retinoic acid (atRA) in human neuroblastoma (SH-SY5Y) cells [5, 6]. The inducible knockdown of *NAV2* in SH-SY5Y cells eliminates atRA-stimulated neurite outgrowth [1].

Human *NAV2* is a homolog of the *C. elegans unc-53* gene [1, 6]. UNC-53 plays an essential role in the longitudinal migration of several cell types including neurons, sex myoblasts and the excretory cell; and mutant alleles of *unc-53* show abnormal mechanosensory neuronal elongation [7, 8]. Ectopic expression of human *NAV2* driven by a mechanosensory neuron

Author to whom all correspondence should be sent: Margaret Clagett-Dame, Ph.D., Department of Biochemistry, University of Wisconsin-Madison, 433 Babcock Dr., Madison, WI, 53706-1544, USA, Phone: 608-262-3450, Fax: 608-262-7122, dame@biochem.wisc.edu.

promoter largely rescues defects in axon elongation in *C. elegans*, thereby demonstrating that NAV2 and UNC-53 are orthologs [1].

A *Nav2/unc53H2* hypomorphic mutant mouse lacking the full-length NAV2 protein shows impaired acuity of several sensory systems including a reduction in the ability to feel pain [9]. *Nav2/unc53H2* mutant embryos show a reduction in overall nerve fiber density, with cranial nerves IX (glossopharyngeal) and X (vagus) sometimes fused or poorly connected to the hindbrain. Additional work from our group shows that the formation of parallel axon fibers and neuronal migration is disrupted in the cerebellum of *Nav2/unc53H2* hypomorphs, and that these mutants exhibit abnormal vermal foliation and ataxia [3].

The *NAV2* open reading frame (ORF) encodes for a protein of 261 kDa with several conserved domains, including a calponin homology (CH) domain, four coiled-coil (CC) domains, a cytoskeletal interacting region (CSID), and an AAA-domain [1]. NAV2 is a member of a family of neuron navigator proteins comprised of NAV1, NAV2, and NAV3 [10]. When expressed in Cos-1 cells, NAV2 staining appears along microtubules, and this profile is disrupted when the microtubule network is de-stabilized [1]. Our group previously identified a region of NAV2 that can independently localize to the microtubule cytoskeleton [1]. This domain is very similar to a microtubule-binding domain (MTBD) identified in NAV1 [11].

Although NAV2 plays a role in axonal elongation and cell migration, the molecular basis for these effects is unknown. The objective of the present study was to identify NAV2 protein interacting partners. A region of NAV2 that interacts with the cytoskeleton was used as the bait in a yeast two-hybrid screen to identify the NAV2-interacting partner, 14-3-3ε. Herein we show that knockdown of 14-3-3ε in SH-SY5Y cells or of the *C. elegans* homolog, *ftt-2*, impairs neuronal process elongation.

Methods

Retinoid

All-*trans* retinoic acid (atRA) was obtained from Spectrum Chemical Co. (New Brunswick, NJ, USA) and was deemed greater than 99% pure by reverse-phase HPLC [12].

Cell culture, transfection, and generation of stable knockdown lines

The SH-SY5Y cell line was maintained as previously described [13]. SH-SY5Y cells were transfected using an Amaxa Nucleofector II (Lonza Group, Switzerland). Cos-1 (ATCC, Manassas, VA) and human embryonic kidney HEK-293FT (Invitrogen) cells were maintained in DMEM (4.5 g/L glucose) with 10% FBS at 37°C with 5% CO_2. Cos-1 and HEK-293FT cells were transfected using Fugene 6 (Roche).

To generate stable knockdown cell lines, SH-SY5Y cells were transfected with 2 μg pooled sh*14-3-3ε* (SC-29588-SH) or scrambled shRNA-containing sh*Control* (SC-108060) plasmids (Santa Cruz), and positive transfectants were selected with puromycin.

Plasmid constructs

NAV2-3XFl in the mammalian expression vector, pIRES, was generated as previously described [6]. Full-length *NAV2* was subcloned into pAcGFP-C1 (Clontech) yielding GFP-*NAV2* with an 18 amino acid spacer. *NAV2 bait* (amino acids 761–1380) was amplified by PCR from *Nav2*-3XFl with upstream 5'-TCCATA**CATATG**AATGTCACCACGGAGATG-3' and downstream 5'-TCC**GTCGAC**ATAGTTGGAAGGGGCCGAGTG-3' primers and cloned into the yeast Gal4 DNA binding domain (DBD)-containing vector pGBKT7 (*CSID2*). The N-terminal NAV2 sequence (N-term-NAV2; amino acids 761–960) was amplified using the same upstream primer as the parent *NAV2 bait* (see above) and downstream 5'-TCC**GTCGAC**GGCAGGTGTGTTGGCATAAGA-3' primer, and C-terminal NAV2 (C-term-NAV2; amino acids 936–1380) was amplified with upstream 5'-TCCATA**CATATG**ACCATAGACAACCTCAGC-3' and the same downstream primer used for the *NAV2 bait* construct. For reverse two-hybrid analysis, the *NAV2 bait* was cloned into the yeast Gal4 activation domain (AD)-containing vector pGADT7-Rec (Clontech). *NAV2 bait*, *N-term-NAV2*, and *C-term-NAV2* were also amplified and subcloned into pIRES-hrGFP-1a.

Full-length human 14-3-3 β and ε isoforms were amplified from SH-SY5Y cDNA and cloned into pGBKT7 for reverse hybrid analysis, and *14-3-3ε* was cloned into pCDNA-3.1/myc-His-A (Invitrogen) to generate a C-terminal *14-3-3ε*-Myc/His-tagged construct. All newly generated plasmids were verified by sequencing, and the *14-3-3* constructs were identical to NCBI sequences U28936 (*14-3-3ε*) and NM_003404 (*14-3-3β*).

Immunocytochemistry

Cells were fixed in methanol for 5 minutes at −20°C or in 4% paraformaldehyde for 15 minutes at room temperature followed by permeabilization with Triton-X-100 (0.25%). Primary antibodies used included anti-flag M2 antibody (1:1000, Sigma Aldrich); anti-c-myc (1:1000, Sigma Aldrich); anti-α tubulin B-5-1-2 (1:500, Cos-1; 1:2000, SH-SY5Y; Sigma Aldrich); anti-α tubulin (1:100 Abcam); anti-GFP (1:500, Millipore); and anti-GFP (1:500, Invitrogen). Secondary antibodies included goat anti-rabbit and goat anti-mouse 488 and 594 Alexa fluor (Invitrogen). Images were acquired using a Nikon A1 laser scanning confocal microscope equipped with Nikon NIS Elements C imaging software at the W.M. Keck Laboratory for Biological Imaging at the University of Wisconsin-Madison. The optical thickness was set at 0.15 um using a Plan Apo VC 60X oil-immersion objective, and images were collected in channel series. A subset of samples were imaged using the OMX 3D-SIM Super-Resolution system (Applied Precision) with a UNIPLANAPRO 60X/1.42 numerical aperature oil objective. Images were processed using softWoRx (Applied Precision).

Evaluation of neurite outgrowth

Images of cells stained with an antibody to α-tubulin were acquired on an inverted Nikon TE 2000 microscope with a CoolSnap EX camera from Photometrics using QED Imaging Software. The neurite outgrowth module in Metamorph v6.3 (Molecular Devices, Downington, PA) was used to measure average neurite length (μm per cell). For each group,

at least 1000 cells were measured representing a minimum of 6 random non-overlapping images per replicate of each treatment condition.

Co-immunoprecipitation and immunoblotting

Transfected HEK-293FT cells were lysed in buffer containing 50 mM Tris-HCl, pH 7.5; 150 mM NaCl; 5 mM EDTA; 1% NP-40; 0.1mM dithiothreitol (DTT) containing protease and phosphatase inhibitors. Cell lysates containing NAV2 protein (NAV2 bait, N-terminal NAV2 or C-terminal NAV2) were incubated with anti-flag mAb (Sigma) or purified mouse IgG (Sigma), followed by precipitation with protein G-agarose beads (Thermo Scientific) blocked with 3% fish skin gelatin. The beads were washed with lysis buffer, and antibody-antigen complexes were removed by boiling in reducing Laemmli sample buffer. Samples were resolved by SDS-PAGE and transferred to nitrocellulose followed by immunoblotting using flag-HRP (1:30,000, Sigma Aldrich), and 6×-His-HRP (1:2000, Clontech) antibody conjugates to detect NAV2 flag-tagged constructs and 14-3-3ε-Myc/His, respectively. Antibody-antigen complexes were detected using the SuperSignal West Pico Chemiluminescent kit (Thermo Scientific) after exposure to X-ray film.

Yeast two-hybrid screening

The construction of an atRA-induced SH-SY5Y prey library and subsequent NAV2 bait screens were carried out using the Matchmaker Library Construction and Screening Kit (Clontech) following the manufacturer's guidelines. The prey library was constructed using poly(A)$^+$ RNA from SH-SY5Y cells treated with 1 μM atRA for 24 hours. Following reverse transcription, a cDNA library of DNA fragments fused to the GAL4 activation domain (AD) in the pGADT7-Rec expression vector was generated. The *NAV2* bait construct in the DBD-containing pGBKT7 vector was transformed into the yeast haploid strain, Y187, mating type α, and the atRA SH-SY5Y cDNA library was transformed in the AH109 mating type A. The bait and prey -containing haploid strains were mated to form diploid yeast colonies containing both vectors. After selection on media lacking leucine, tryptophan, histidine and adenine (SD/-Trp/-Leu/-His/-Ade), DNA was isolated from individual colonies using the Zymoprep Yeast Plasmid Miniprep Kit I (Zymo Research) following the manufacturer's guidelines. Isolated yeast DNA (5 μl) was transformed into electrocompetent XL1 Blue cells. NAV2 interacting partner identities were determined by sequence analysis using the pGADT7-Rec 3' internal sequencing primer (upstream 5'-TAATACGACTCACTATAGGG-3') and BLAST searches against the human genome (NCBI; http://blast.ncbi.nlm.nih.gov/Blast.cgi).

C. elegans strains

C. elegans strains were maintained according to standard protocols [14]. Strains used in this study include: EG1194 (*lin-15(n765ts);oxls1[pmec-7::gfp;lin-15(+)*]), *eri-1(mg366), eri-1(mg366);oxls1, ftt-2(n4426), and ftt-2(n4426);oxls1*.

RNA interference and mutant analysis

EG1194 (*lin-15(n765ts);oxls1*[P*mec-7::*GFP*;lin-15*(+)]) *C. elegans* were crossed with *eri-1(mg366)* [15] to generate *eri-1(mg366);oxls1* expressing GFP in the mechanosensory

neurons. In the EG1194 strain, GFP in the mechanosensory neuron is driven by the integrated *pmec-7::gfp* reporter allowing direct observation of the PLM neurons using fluorescent microscopy. This stain was crossed with the *eri-1(mg366)* strain to enhance the effects of dsRNAs in neurons. RNAi was fed according to standard protocols [16]. L3 progeny were measured from at least three separate RNAi experiments and PLM length was determined as previously described [1]. *Pos-1* was used as a positive control, and the number of eggs hatched over the number of eggs not hatched served as a measure of penetrance (*pos-1* RNAi feeding causes eggs laid not to hatch). The negative control was the empty feeding vector (L4440). The PLM was scored as abnormal if its most anterior axonal extension was shorter than the lowest 1% of the PLMs of the negative control (empty RNAi feeding vector).

In C. elegans *ftt-2* encodes for a 14-3-3-like protein [17]. EG1194 (*lin-15(n765ts);oxls1*[P*mec-7::*GFP*;lin-15*(+)]) *C. elegans* were crossed with *ftt-2(n4426) C. elegans* to generate *ftt-2(n4426);oxls1*[P*mec-7::*GFP*;lin-15*(+)] expressing GFP in the mechanosensory neurons. The PLM was measured as described above and scored as abnormal if the PLM failed to reach the lower limits (≤ 1%) of an EG1194 PLM.

Results

Identification of 14-3-3 isoforms as NAV2 protein interacting partners

In order to identify NAV2 protein interacting partners, five GAL4 DNA binding domain (DBD)-NAV2 fusion constructs spanning the NAV2 sequence were used as bait to screen a atRA-induced SH-SY5Y cDNA prey library (Fig S1). The bait construct containing amino acids 761 to 1380 identified 14-3-3ε and β isoforms as candidate NAV2 interacting partners at high frequency (10.3% and 3.1% of all positives, respectively) (Fig. 1 and Fig. S1). This region of NAV2 spans the previously identified cytoskeletal domain in the full-length protein [1] and when expressed in Cos-1 cells, shows an overlapping distribution with α-tubulin (Fig. S2 A–C). The distribution of the bait construct is similar to that of the full-length protein that also associates with the cell cytoskeleton (Fig. S2, D–F & G–I). Given the importance of 14-3-3ε in neuronal migration and brain development [18], we focused our attention on confirming this interaction with NAV2. Using a reverse two-hybrid screen in which the GAL4 AD was fused to NAV2 bait (AD-NAV2) and the 14-3-3 isoforms were fused to the GAL4 DBD (DBD-14-3-3 ε or β; Fig. 1C), the interaction between the NAV2 protein and both 14-3-3β and 14-3-3ε was confirmed. Once the interaction was verified, 14-3-3ε served as the focus of additional studies.

In order to more precisely map the interface of NAV2 required for interaction with 14-3-3ε, N-terminal and C-terminal NAV2 deletion constructs were prepared and tested in the two-hybrid assay. The 620 amino acid NAV2 bait sequence comprises 25.5% of the full-length 261 kDa NAV2 protein. From this, two smaller constructs were generated, one comprised of the first 200 amino acids (N-terminal; 761–960) and another contained the C-terminal amino acids 936–1380 (Fig. 2A). When the intact NAV2 bait construct was tested with the full-length 14-3-3ε protein, mated colonies had the expected reporter activity (96.1%). Similar activity was observed when the N-terminal construct was screened against the 14-3-3ε isoform (93.6%), whereas all reporter activity was lost with the C-terminal region (Fig. 2B).

Following expression in mammalian cells, a co-immunoprecipitation assay was used as a second means to confirm the specific interaction of 14-3-3ε with the N-terminal region of the NAV2 bait (Fig. 2C). Full-length 14-3-3ε-Myc/His was detected at 36 kDa by immunoblotting with the His(6×) antibody after immunoprecipitation using either the intact NAV2 Bait-3×Fl or the N-term-NAV2-3×Fl bound to flag antibody-coated agarose beads. In contrast, the 14-3-3ε-Myc/His protein was not pulled down when co-transfected with C-term-NAV2. No 14-3-3ε-Myc/His protein was detected when co-transfected with any of the NAV2 constructs when mouse IgG was immobilized in place of the anti-flag antibody on the agarose beads. Thus, the region of NAV2 required for interaction with the 14-3-3ε protein was localized to 200 amino acids within the N-terminus of the original NAV2 bait, and corresponds to 7.3% of the protein encoded by the full-length 261 kDa NAV2 ORF.

NAV2 and 14-3-3ε are distributed similarly in cells

Immunofluorescence studies of full-length NAV2 containing either a C-terminal flag or N-terminal GFP sequence, and 14-3-3ε tagged with Myc/His were conducted in Cos-1 cells. 14-3-3ε-Myc/His alone was most highly expressed in the cytoplasm adjacent to the nucleus, where the highest staining for α-tubulin, a microtubule component, was also noted (Fig. S3). NAV2-3×Fl and GFP-NAV2 staining was observed adjacent to the nucleus and in a punctate pattern along cell processes, overlapping that of α-tubulin immunofluorescence (Fig. S2, D–F & G–I). When expressed together, 14-3-3ε and NAV2 co-localized along the cytoskeleton (Fig. 3 A–C and D–F). These results were confirmed by structured illumination microscopy (Fig. 3 G–I). Analysis of 14-3-3ε-Myc/His and GFP-NAV2 staining in the human neuroblastoma cell (SH-SY5Y) showed overlap at the juncture of the cell leading into the neurite (hillock) and at varicosities along the neurite (Fig. S4). Thus, the full-length NAV2 and 14-3-3ε proteins localize together when co-expressed in cells.

14-3-3ε knockdown reduces the ability of atRA to induce neurite outgrowth

In SH-SY5Y cells, *NAV2* mRNA is induced by atRA [6] and knockdown eliminates atRA-induced neurite outgrowth [1]. In order to determine whether the induction of neurite outgrowth in SH-SY5Y cells by atRA also requires 14-3-3ε, a stable knockdown line was generated using a pool of shRNAs targeted to *14-3-3ε*. There was no significant difference in mean neurite length between the vehicle-treated sh*Control* and sh*14-3-3ε* cell lines (Figure 4A, open bars). In contrast, treatment of the sh*Control* cell line with atRA produced a robust increase in neurite length, whereas the effect of atRA on neurite length in the 14-3-3ε knockdown cells was significantly blunted (Figure 4A, compare the filled bars).

FTT-2 plays a role in PLM neuron axon elongation

Members of the 14-3-3 protein family are highly conserved across species [19–23], and evaluation of the *C.elegans* database revealed two potential homologs of 14-3-3ε, FTT-2 (68% identical and 80% similar) and FTT-1 (66% identical and 78% similar). RNAi-mediated depletion of FTT-2 resulted in posterior lateral mechanosensory (PLM) length defects comparable to those observed with depletion of UNC53, the NAV2 ortholog found in *C. elegans*. Because knockdown of FTT-1 causes a strong sterile phenotype [24,25], studies of this homolog were not pursued. Thus, both RNAi mediated reduction of FTT-2

and UNC-53 leads to a shortening of the PLM axonal processes as compared to the RNAi control (Fig. 5A).

PLM length was also examined in the *ftt-2* mutant, *ftt-2(n4426)*, in which the promoter and part of the first exon including the start codon is deleted [17]. As observed with RNAi, an increased number of the *ftt-2(n4426);oxls1* PLM neurons were truncated compared to the control EG1194 *C. elegans* strain (11.6 % versus 1.0%; Fig. 5B & 5C). Thus, experimental evidence supports a role for the 14-3-3 homolog *ftt-2* in elongation of the PLM neuron.

Discussion

In this study 14-3-3ε is identified as a NAV2 interacting partner. Using two model systems, we have shown that both proteins play a role in neuronal elongation. In SH-SY5Y cells, a reduction in 14-3-3ε protein impairs neurite outgrowth in response to atRA, an effect previously observed in NAV2 knockdown cells [1]. In *C. elegans*, knockdown of FTT-2 produces PLM elongation defects mirroring those observed with the depletion of UNC-53.

NAV2 contains multiple promoters, and alternative splicing of RNA transcripts has been reported [6, 9]. It is the long isoform of *NAV2* encoding for a protein of 261 kDa that is induced by atRA and participates in neurite outgrowth in human neuroblastoma cells [1]. The long *Nav2* isoform is also the major form expressed in neural tissues during embryonic development and in the adult nervous system [6, 9, 26, 27]. The region of NAV2 that interacts with 14-3-3ε (amino acids 761 to 960) lies in a region that is absent in the putative short NAV2 isoforms. Thus, our current findings are consistent with a role for 14-3-3ε participating with the long NAV2 isoform to support atRA-induced neurite outgrowth in SH-SY5Y cells and elongation of the PLM neuron in *C. elegans*.

14-3-3 proteins are conserved from bacteria to humans and are highly expressed in the mammalian nervous system [19–21, 23, 28]. They bind to a large number of partners and function in diverse processes including signal transduction, cell cycle regulation, and apoptosis. They can regulate enzyme activity, direct the subcellular localization of proteins, and function as adaptor molecules, regulating protein-protein interactions. It has been previously demonstrated that 14-3-3ε is necessary for proper neuronal migration *in vivo* [18]. 14-3-3ε interacts with phosphorylated NUDEL, which in turn, interacts with LIS1 forming a complex that is found near the centrosome and is also transported into axons [18, 29, 30]. NUDEL and LIS1 interact with the microtubule motor, cytoplasmic dynein heavy chain, to regulate centrosomal protein location as well as microtubule dynamics, and the complex is essential for neuronal migration [30, 31]. 14-3-3ε deficiency results in mis-localization of the NUDEL/LIS complex [18]. It is possible that NAV2 binding to 14-3-3ε could influence its ability to bind to NUDEL. Alternatively, NAV2 could serve a scaffolding/enzymatic role, bringing additional functional proteins to the complex, or possibly by integrating signaling cues to other components of the cytoskeleton [2]. Interestingly, LIS1-deficient cerebellar granule neurons are defective in axonal extension and neuronal migration [32], an effect also observed in EGL explants and neurons cultured from *Nav2/unc53H2* hypomorphic mutant mice [3]. The present work showing that NAV2 interacts with 14-3-3ε suggests that NAV2 could participate in regulating cytoskeletal

dynamics as a part of protein complexes that also contain 14-3-3ε. However, we cannot exclude the possibility that NAV2 and 14-3-3ε function in distinct cellular pathways to influence neurite/axonal outgrowth.

In summary, we show that NAV2 interacts with 14-3-3ε, and when over-expressed in Cos-1 cells, NAV2 and 14-3-3ε localize together. Knockdown of either 14-3-3ε or NAV2 in human neuroblastoma cells results in a reduction in atRA-mediated neurite outgrowth, whereas reduction of 14-3-3ε (FTT-2) or NAV2 (UNC-53) in *C. elegans*, produces a reduction in mechanosensory (PLM) axonal elongation suggesting the function of these two proteins is evolutionarily conserved. Future studies will be directed at identifying the importance of 14-3-3ε/NAV2 interaction in neuronal cell process elongation and migration, as well as towards understanding the networks in which these proteins participate to achieve their effects.

Supplementary Material

Refer to Web version on PubMed Central for supplementary material.

Acknowledgments

TM was supported in part by a fellowship from the Molecular and Applied Nutrition Training program (T32-DK007665). We thank A Mitzey for her help in cell culture and microscopy experiments. We also thank L Vanderploeg in the Biochemisty Media Group for her assistance in preparing the artwork, and L Rodenkirch of the W.M. Keck Laboratory for Biological Imaging for his assistance in confocal microscopy.

References

1. Muley PD, McNeill EM, Marzinke MA, Knobel KM, Barr MM, Clagett-Dame M. The atRA-responsive gene neuron navigator 2 functions in neurite outgrowth and axonal elongation. Dev Neurobiol. 2008; 68:1441–1453. [PubMed: 18726912]
2. Stringham EG, Schmidt KL. Navigating the cell: UNC-53 and the navigators, a family of cytoskeletal regulators with multiple roles in cell migration, outgrowth and trafficking. Cell Adh Migr. 2009; 3:342–346. [PubMed: 19684480]
3. McNeill EM, Klockner-Bormann M, Roesler EC, Talton LE, Moechars D, Clagett-Dame M. Nav2 hypomorphic mutant mice are ataxic and exhibit abnormalities in cerebellar development. Dev Biol. 2011; 353:331–343. [PubMed: 21419114]
4. McNeill EM, Roos KP, Moechars D, Clagett-Dame M. Nav2 is necessary for cranial nerve development and blood pressure regulation. Neural Dev. 2010; 5:6. [PubMed: 20184720]
5. Merrill RA, Ahrens JM, Kaiser ME, Federhart KS, Poon VY, Clagett-Dame M. All-*trans* retinoic acid-responsive genes identified in the human SH-SY5Y neuroblastoma cell line and their regulated expression in the nervous system of early embryos. Biol Chem. 2004; 385:605–614. [PubMed: 15318809]
6. Merrill RA, Plum LA, Kaiser ME, Clagett-Dame M. A mammalian homolog of *unc-53* is regulated by all-*trans* retinoic acid in neuroblastoma cells and embryos. Proc Natl Acad Sci U S A. 2002; 99:3422–3427. [PubMed: 11904404]
7. Hekimi S, Kershaw D. Axonal guidance defects in a *Caenorhabditis elegans* mutant reveal cell-extrinsic determinants of neuronal morphology. J Neurosci. 1993; 13:4254–4271. [PubMed: 8410186]
8. Stringham E, Pujol N, Vandekerckhove J, Bogaert T. *unc-53* controls longitudinal migration in *C. elegans*. Development. 2002; 129:3367–3379. [PubMed: 12091307]

9. Peeters PJ, Baker A, Goris I, Daneels G, Verhasselt P, Luyten WH, Geysen JJ, Kass SU, Moechars DW. Sensory deficits in mice hypomorphic for a mammalian homologue of unc-53. Brain Res Dev Brain Res. 2004; 150:89–101.
10. Maes T, Barceló A, Buesa C. Neuron navigator: a human gene family with homology to *unc-53*, a cell guidance gene from *Caenorhabditis elegans*. Genomics. 2002; 80:21–30. [PubMed: 12079279]
11. Martinez-López MJ, Alcántara S, Mascaró C, Pérez-Brangulí F, Ruiz-Lozano P, Maes T, Soriano E, Buesa C. Mouse neuron navigator 1, a novel microtubule-associated protein involved in neuronal migration. Mol Cell Neurosci. 2005; 28:599–612. [PubMed: 15797708]
12. Motto MGF, K I, Hamburg PF, Burinsky DJ, Dunphy R, Oyler AR, Cotter ML. Separation and identification of retinoic acid photoisomers. J Chromatogr. 1989; 481:255–262.
13. Clagett-Dame M, Verhalen TJ, Biedler JL, Repa JJ. Identification and characterization of all-*trans*-retinoic acid receptor transcripts and receptor protein in human neuroblastoma cells. Arch Biochem Biophys. 1993; 300:684–693. [PubMed: 8382032]
14. Brenner S. The genetics of *Caenorhabditis elegans*. Genetics. 1974; 77:71–79. [PubMed: 4366476]
15. Kennedy S, Wang D, Ruvkun G. A conserved siRNA-degrading RNase negatively regulates RNA interference in *C-elegans*. Nature. 2004; 427:645–649. [PubMed: 14961122]
16. Ahringer, J. WormBook, The *C. elegans* Research Community. 2006. Reverse genetics. http://www.wormbook.org.
17. Berdichevsky A, Viswanathan M, Horvitz HR, Guarente L. SIR-2.1 interacts with 14-3-3 proteins to activate DAF-16 and extend life span. Cell. 2006; 125:1165–1177. [PubMed: 16777605]
18. Toyo-oka K, Shionoya A, Gambello MJ, Cardoso C, Leventer R, Ward HL, Ayala R, Tsai LH, Dobyns W, Ledbetter D, Hirotsune S, Wynshaw-Boris A. 14-3-3epsilon is important for neuronal migration by binding to NUDEL: a molecular explanation for Miller-Dieker syndrome. Nat Genet. 2003; 34:274–285. [PubMed: 12796778]
19. Aitken A. 14-3-3 and its possible role in co-ordinating multiple signalling pathways. Trends Cell Biol. 1996; 6:341–347. [PubMed: 15157431]
20. Aitken A. 14-3-3 proteins: A historic overview. Seminars Cancer Biol. 2006; 16:162–172.
21. Aitken A, Collinge DB, van Heusden BP, Isobe T, Roseboom PH, Rosenfeld G, Soll J. 14-3-3 proteins: a highly conserved, widespread family of eukaryotic proteins. Trends Biochem Sci. 1992; 17:498–501. [PubMed: 1471260]
22. Roseboom PH, Weller JL, Babila T, Aitken A, Sellers LA, Moffett JR, Namboodiri MA, Klein DC. Cloning and characterization of the epsilon and zeta isoforms of the 14-3-3 proteins. DNA Cell Biol. 1994; 13:629–640. [PubMed: 8024705]
23. Skoulakis EM, Davis RL. 14-3-3 proteins in neuronal development and function. Mol Neurobiol. 1998; 16:269–284. [PubMed: 9626666]
24. Morton DG, Shakes DC, Nugent S, Dichoso D, Wang W, Golden A, Kemphues KJ. The *Caenorhabditis elegans par-5 gene* encodes a 14-3-3 protein required for cellular asymmetry in the early embryo. Dev Biol. 2002; 241:47–58. [PubMed: 11784094]
25. Li J, Tewari M, Vidal M, Lee SS. The 14-3-3 protein FTT-2 regulates DAF-16 in *Caenorhabditis elegans*. Dev Biol. 2007; 301:82–91. [PubMed: 17098225]
26. Coy JF, Wiemann S, Bechmann I, Bachner D, Nitsch R, Kretz O, Christiansen H, Poustka A. Pore membrane and/or filament interacting like protein 1 (POMFIL1) is predominantly expressed in the nervous system and encodes different protein isoforms. Gene. 2002; 290:73–94. [PubMed: 12062803]
27. Ishiguro H, Shimokawa T, Tsunoda T, Tanaka T, Fujii Y, Nakamura Y, Furukawa Y. Isolation of HELAD1, a novel human helicase gene up-regulated in colorectal carcinomas. Oncogene. 2002; 21:6387–6394. [PubMed: 12214280]
28. Tzivion G, Avruch J. 14-3-3 proteins: active cofactors in cellular regulation by serine/threonine phosphorylation. J Biol Chem. 2002; 277:3061–3064. [PubMed: 11709560]
29. Niethammer M, Smith DS, Ayala R, Peng J, Ko J, Lee MS, Morabito M, Tsai LH. NUDEL is a novel Cdk5 substrate that associates with LIS1 and cytoplasmic dynein. Neuron. 2000; 28:697–711. [PubMed: 11163260]

30. Sasaki S, Shionoya A, Ishida M, Gambello MJ, Yingling J, Wynshaw-Boris A, Hirotsune S. A LIS1/NUDEL/cytoplasmic dynein heavy chain complex in the developing and adult nervous system. Neuron. 2000; 28:681–696. [PubMed: 11163259]

31. Wynshaw-Boris A, Pramparo T, Youn YH, Hirotsune S. Lissencephaly: Mechanistic insights from animal moedls and potential therapeutic strategies. Seminars Cell Dev Biol. 2010; 21:823–830.

32. Kholmanskikh SS, Dobrin JS, Wynshaw-Boris A, Letourneau PC, Ross ME. Disregulated RhoGTPases and actin cytoskeleton contribute to the migration defect in Lis1-deficient neurons. J Neurosci. 2003; 23:8673–8681. [PubMed: 14507966]

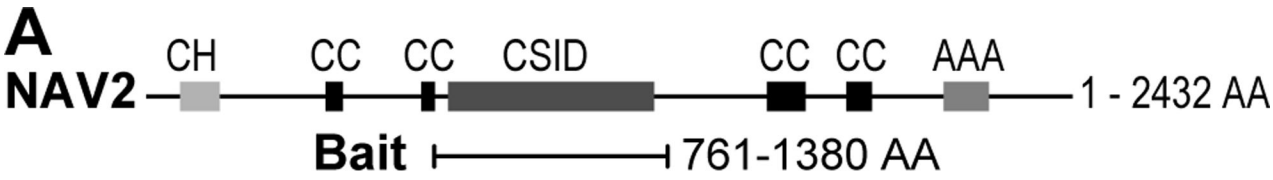

B

Bait	MW (kDa)	Y2H Mating Efficiency (%)	Interacting Partner	Frequency
NAV2	68.1	17.7%	14-3-3ε 14-3-3β	10.3% (10/97) 3.1% (3/97)

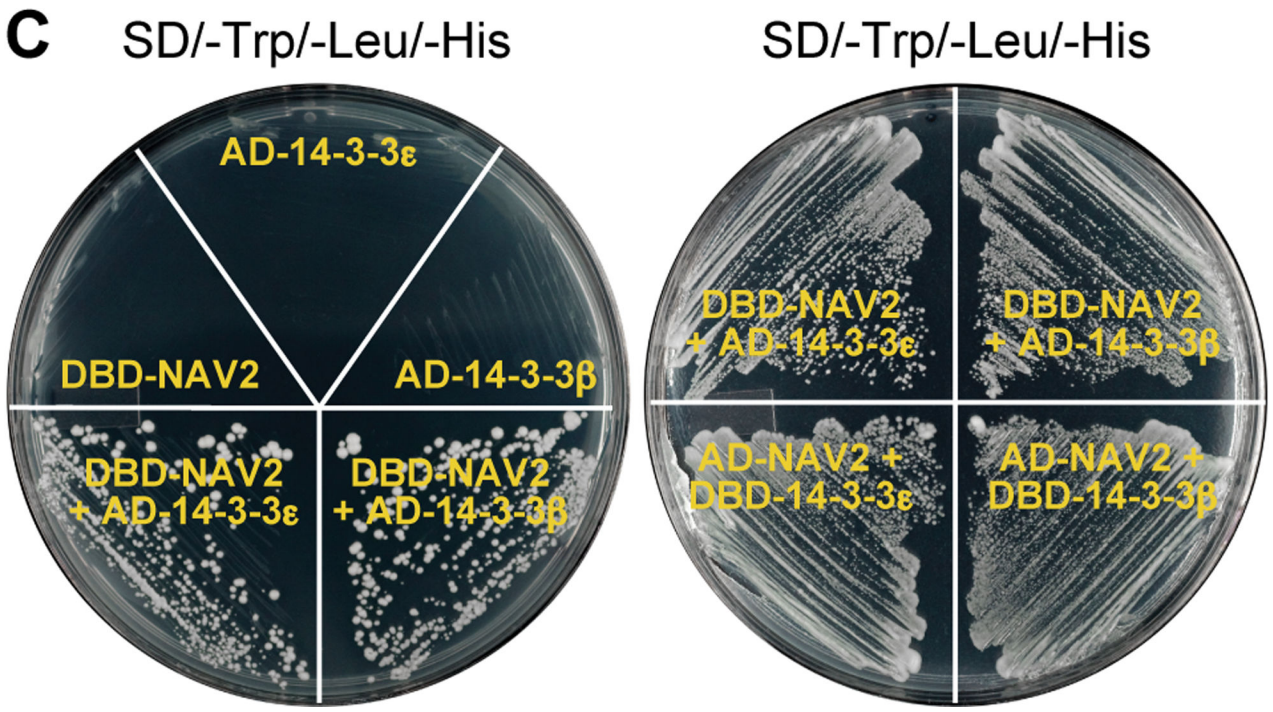

Figure 1. Identification of 14-3-3 isotypes as novel NAV2 interacting partners

(**A**) Schematic showing the location of the NAV2 bait in the full-length NAV2 protein. (**B**) Identification of 14-3-3ε and β isoforms as NAV2 interacting partners from the genetic yeast two-hybrid screen. Frequency was calculated by dividing the number of times the candidate was identified by the total number of selected yeast colonies on minimal media lacking leucine (-Leu), tryptophan (-Trp), and histidine (-His). (**C**) Images of colonies growing on plates illustrating the interaction between NAV2 and 14-3-3 isoforms. On the plate shown on the left, there is no growth on SD/-Leu/-Trp/-His dropout plates when yeast express

either the NAV2 DBD fusion or AD-14-3-3 protein alone, but in diploid yeast containing both, yeast growth occurs. The plate on the right shows both two hybrid (plate-top) and reverse two-hybrid (plate-bottom) analysis of the NAV2 interaction with each of the 14-3-3 isoforms. There is growth on SD/-Leu/-Trp/-His plates of mated yeast containing either DBD-NAV2 and AD-14-3-3ε or β and AD-NAV2 and DBD-14-3-3ε or β. CH, calponin homology domain; CC, coiled coil domains; CSID, cytoskeletal interacting domain; AAA, AAA-ATPase domain

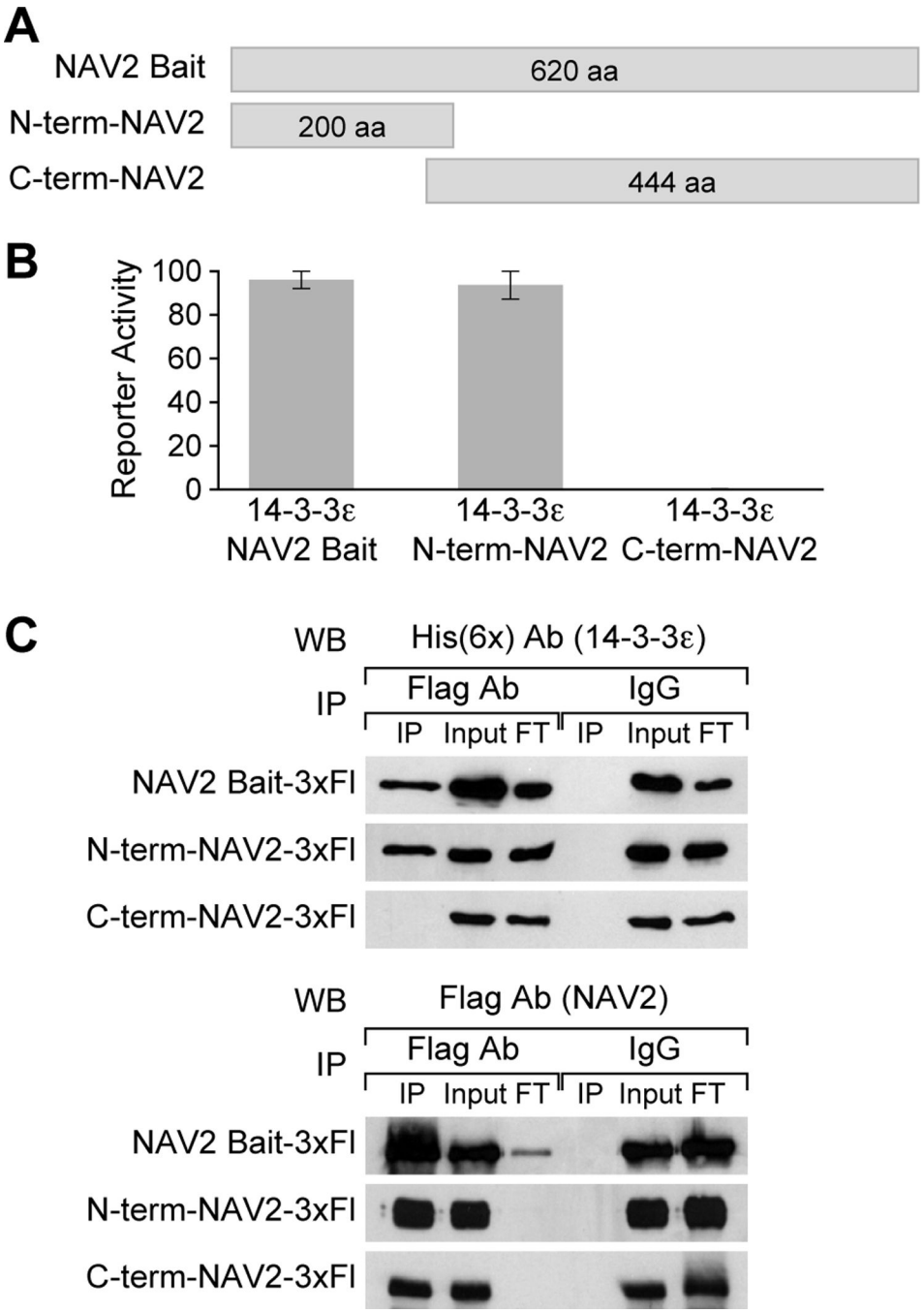

Figure 2. The amino terminal region of the NAV2 bait protein interacts with 14-3-3ε

(**A**) Schematic of the intact NAV2 bait (aa 761–1380), N-term-NAV2 (aa 761–961) and C-term-NAV2 (aa 936–1380). (**B**) Reporter activity in in yeast containing14-3-3ε and either the entire NAV2-bait, N-term- or C-term NAV2 construct. The N-term-NAV2 activity equals that of the original NAV2 bait, whereas no activity is observed with the C-term-NAV2 construct. Reporter activity is defined as the frequency of mated colonies that grow on SD/-Trp/-Leu/-His. (**C**) Immunoprecipitation of 14-3-3ε-Myc/His protein by NAV2 constructs. 293HEK-FT cells were co-transfected with NAV2 bait-3×Fl, N-term-

NAV2-3×Fl or C-term-NAV2-3×Fl along with 14-3-3ε-Myc/His, and immunoprecipitated with monoclonal anti-flag antibody or mouse IgG as a control. Samples of the cell lysates (input), flow through (FT) and immunoprecipitate (IP) were resolved by SDS-PAGE, and transferred to nitrocellulose. Immunoblotting was performed with antibodies against flag to detect NAV2 proteins and His(6×) to detect 14-3-3ε. The 14-3-3ε protein was pulled down both by the NAV2 bait-3×Fl and N-term-NAV2-3×Fl, whereas it did not interact with the C-term-NAV2-3×Fl.

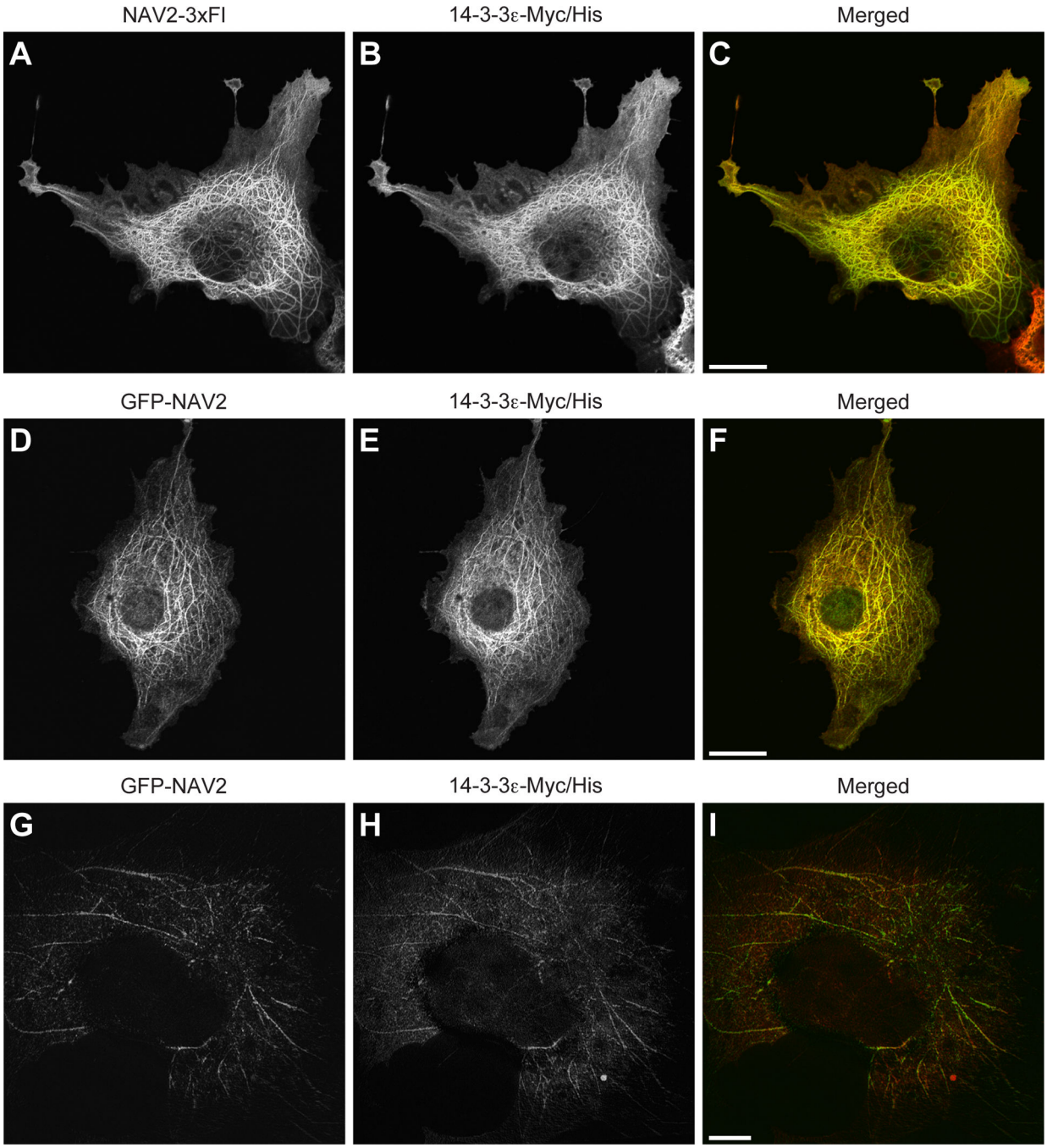

Figure 3. Full-length NAV2 and 14-3-3ε distribute similarly in cells

A–C. Confocal analysis of full-length NAV2-3×Fl and GFP-NAV2 proteins co-expressed with 14-3-3ε-Myc/His in Cos-1 cells (**A–C** and **D–F**). Both NAV2-3×Fl (**A**) and 14-3-3ε-Myc/His (**B**) localize in similar regions of the cell (**C**). Likewise, when NAV2 is tagged at the N-terminus with GFP (GFP-NAV2, **D**) and co-expressed with 14-3-3ε-Myc/His (**E**), the proteins distribute together (**F**). (**G–H**) The cellular distribution of GFP-NAV2 and 14-3-3ε-Myc/His using Super-Resolution microscopy (SIM) is shown in panels G–I. When images

captured by SIM were analyzed in Fiji/ImageJ, Manders' threshold coefficients for M1 and M2 of 0.653 and 0.752, respectively, were obtained. (Scale bar = 20 μm).

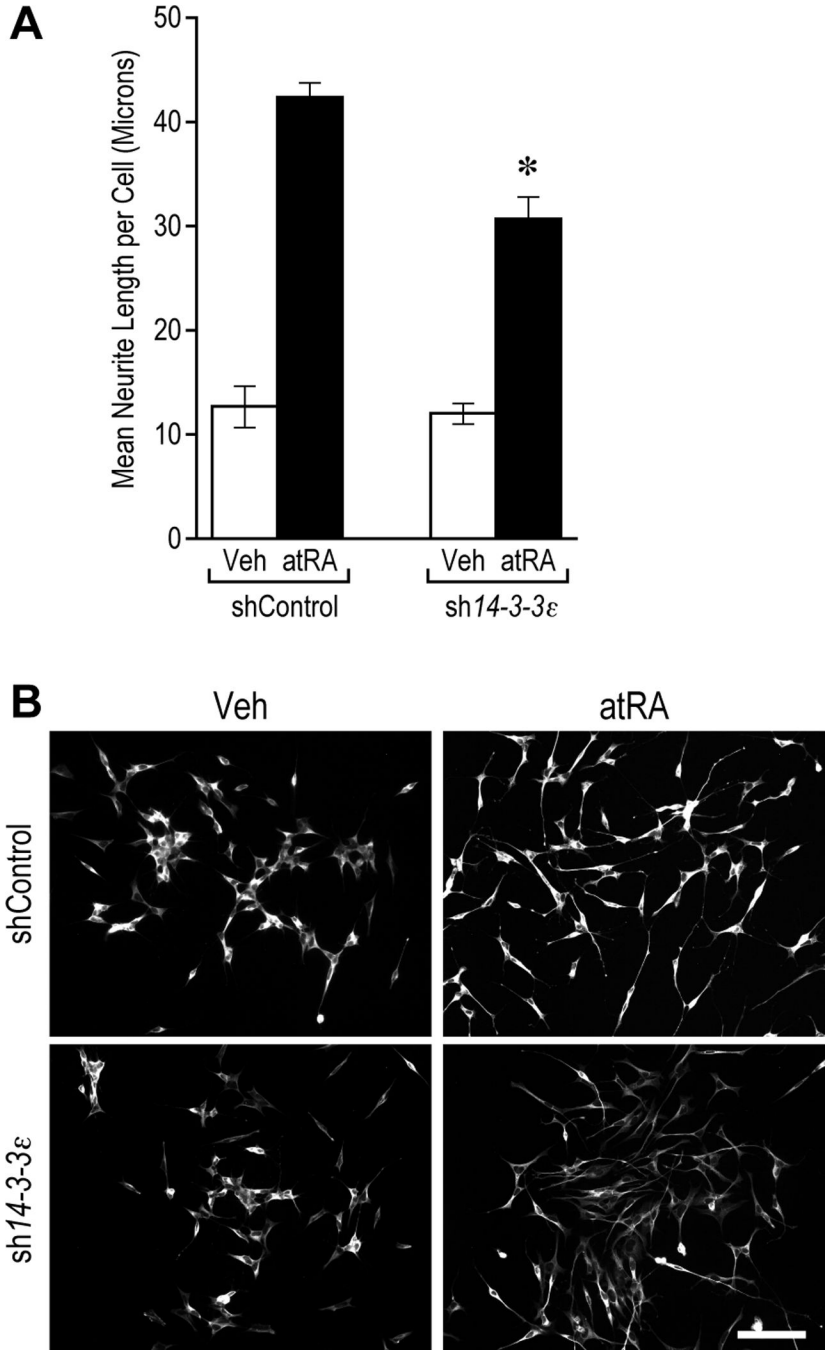

Figure 4. *14-3-3ε* knockdown reduces atRA-induced neurite outgrowth

(**A**) shControl and *14-3-3ε* knockdown cells were treated with atRA and the effect on mean neurite length was assessed after 48h. The asterisk indicates a significant difference between atRA-treated shControl and atRA-treated sh-*14-3-3ε* at $p < 0.05$. Results are mean ± standard error. Analysis of mRNA and protein showed an approximate 30–50% reduction in the sh-*14-3-3ε* cell line (data not shown), suggesting the inability of knockdown to more fully eliminate atRA-induced neurite outgrowth may be explained by the 14-3-3ε protein that remains. (**B**) SH-SY5Y cell morphology after exposure to vehicle or atRA. Cells were

fixed, and stained using an antibody to α-tubulin. The results shown are representative of at least two independent experiments. (Scale bar = 100 μm).

A

RNAi	Percentage of truncated PLM axons	n
Control	0.9	1 / 16
ftt-2	11.5	15 / 130
unc-53	22.0	26 / 118

B

Mutant	Percentage of truncated PLM axons	n
Control	1.0	2 / 197
ftt-2	11.6	28 / 242

C

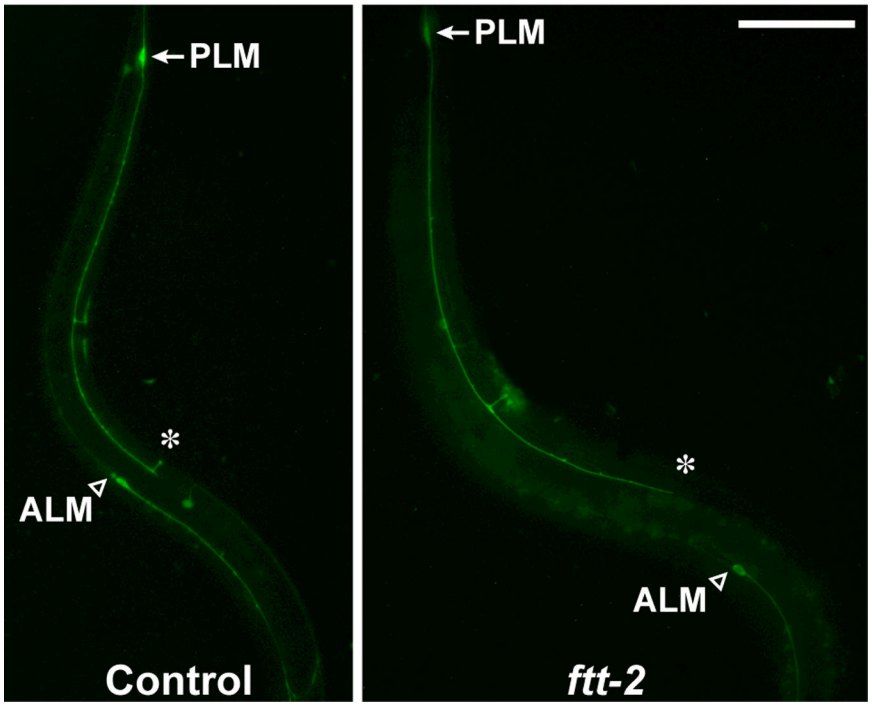

Figure 5. Mechanosensory axon length is reduced with *unc-53* and *ftt-2* RNAi feeding, and in the *ftt-2 C. elegans* mutant

(**A**) Effect of RNAi feeding on on PLM axon length. RNAi feeding experiments were performed in EG1194 crossed with *eri-1(mg366)* [15], a strain that is more sensitive to the effects of RNAi in neurons. PLM neurons were scored as abnormal if they failed to reach the lower 1% of worms fed the empty RNAi vector (L4440, control). (**B**) Percentage of PLM axons truncated in *ftt-2* (*n4426*) mutant animals carrying the integrated *pmec-7::gfp* transgene. (**C**) Representative fluorescence images of control (EG1194) and *ftt-2* (*n4426*);

oxls1 transgene animals. PLM, posterior lateral mechanosensory neuron cell body (white arrow, filled); ALM, anterior lateral mechanosensory neuron cell body (open arrow head). The asterisk (*) indicates the anterior limit of extension of the PLM axon. (Scale bar = 50 μm).